Influence of Ionic Groups on the Crystallization and Melting Behavior of Segmented Polyurethane Ionomers

Y. Zhu, J. L. Hu, K. W. Yeung, Y. Q. Liu, H. M. Liem

Institute of Textiles and Clothing, The Hong Kong Polytechnic University, Hung Hum, Kowloon, Hong Kong, Republic of China

Received 1 June 2005; accepted 22 August 2005
DOI 10.1002/app.23009
Published online in Wiley InterScience (www.interscience.wiley.com).

ABSTRACT: The isothermal crystallization kinetics and melting behavior of the soft segment in polyurethane (PU) ionomer/nonionomer based on PCL-4000 (poly(ε-caprolactone)) were investigated using polarizing optical microscopy (POM) and differential scanning calorimetry (DSC). In general, the presence of ionic groups in PU ionomers can promote the formation of a more stable crystalline structure and lower the equilibrium melting temperature of the crystallizable phase. Comparison between the crystallization characteristics of PU nonionomers and ionomers suggests that the Coulombic Forces between ionic groups within hard segment can increase the crystallization rate and decrease the crystal size of soft segment when the total molecular weight (M_w) of PU ionomer is higher than ~71,000. On the other hand, the opposite effect of ionic groups on the crystallization rate is observed in PU ionomers with M_w below ~20,000. The DSC thermograms illustrate that the ionic groups can significantly enhance the microphase separation in PU ionomers with higher M_w values. By the control and manipulation of crystallization and microstructure formation in PU ionomer, it is possible to achieve shape memory PUs with superior physical property. © 2006 Wiley Periodicals, Inc. J Appl Polym Sci 100: 4603–4613, 2006

Key words: polyurethanes; ionomers; phase separation; isothermal crystallization; melting behavior

INTRODUCTION

Segmented PUs are thermoplastic block copolymers having a wide range of glass transition temperatures. Foremost among the unique mechanical properties of this class of copolymers are the pseudoelasticity and thermal-responsive shape memory effect. Because of the presence of soft and hard segments, the former comprises the reversible phase, while the latter forms the frozen phase: the material can restore its original shape upon heating above certain temperature T_s (melting point of soft segment) after being strained. This unique feature of this type of material has aroused serious research interests, both academia and industry, in recent two decades.[1–9] Li et al. have investigated the relations between the shape memory effect and molecular structure of segmented PU with PCL as the soft segment.[10,11] The authors concluded that high crystallinity of the soft segment regions at room temperature was a necessary prerequisite for the segmented copolymers to demonstrate shape memory behavior. Accordingly, a lower limit of PCL molecular weight (~2000–3000) below which the PCL segments were not able to crystallize at the usual processing conditions was then established. The immediate conclusion is that crystallization plays an important role on the shape fixation in segmented PU. In addition, it was observed by Bogdanow and coworkers that the crystallinity, crystallization rate, and the physical mobility of the PCL soft segment during crystallization depend upon the hard segment concentration, length of the soft segment, and total molecular weight of the block copolymer (poly(ether urethanes) (PEUs) in their case).[12] Taking into account these interrelated parameters, the authors concluded that (i) crystallization was inhibited by the shortening of the crystallizable block resulting from the enhanced number of interconnections between soft and hard segments, and (ii) crystallizability of the PEUs was inversely proportional to the total molecular weight of the polymer: the highest degree of crystallinity can be achieved in the lowest molecular weight PEUs. Therefore, it can be concluded that the soft segment length, hard segment content, and the total molecular weight play the important roles on the crystallization of the crystallizable soft phase in segmented PU.

In recent years, numerous studies on PU ionomers are emerging because of their superior mechanical and thermal properties. For example, tensile strength, modulus, elongation at fracture, etc., of the PU ionomers in the form of thin films increased due to the presence of Coulombic Forces between the ionic cen-

Correspondence to: J. L. Hu (tchujl@inet.polyu.edu.hk).
Contract grant sponsor: Innovation Technology Fund, Hong Kong; contract grant number: ITS/098/02.

TABLE I
Formulation of the Synthesis of Polyurethane Samples

Sample	PCL (wt %)[a]	DMPA (wt %)[b]	Soft segment (mol)	Hard segment (mol)			M_w	M_w/M_n
			PCL-4000	MDI	DMPA	BDO[c]		
PU-20N PU-20I	80.0	5.00%	0.34	1	0.63	0.03	20,200	3.2
PU-58N PU-58I	80.0	5.00%	0.34	1	0.63	0.03	58,500	4.7
PU-71N PU-71I	80.0	5.00%	0.34	1	0.63	0.03	71,600	3.7

[a] Mass content of soft segments in PU samples.
[b] Mass content of DMPA in PU samples.
[c] BDO content can change slightly to obtain different M_w values.

ters within the polymer backbone.[13–15] Kim et al.[15] have demonstrated the existence of shape memory effect in segmented PU ionomers based on PCL, with various structural parameters such as soft segment length, hard segment content, and ionic group content. Their DSC result indicated that for PCL-4000 (M_w = 4000) based PUs with 70% soft segment content, the PU nonionomers and ionomers showed similar thermal behavior, except that the nonionomers were of slightly lower ΔH_{cs} (heat of crystallization) and ΔH_{fs} (heat of fusion), implying an enhancement of the microphase separation in the ionomers. However, when the soft segment content is 55% and of the same soft segment length, its crystallization is observed in solely nonionomers but not in ionomers. Accordingly, it is concluded that the twofold effect of ionic groups within hard segments exists and the molecule is of different physical structure. As a result, the microphase separation has different morphologies, leading to diverse soft segment crystallization, which greatly affects the shape memory property. In general, the effect of ionic groups on the crystallization of soft segment cannot be ignored especially for segmented PU with different molecular weights. This effect can thus be utilized as the design guidance for novel segmented PU ionomers having unique physical property.

In this study, segmented PU ionomers, having PCL as the soft segment, with different molecular structures have been synthesized and investigated. The introduction of ionic groups to the hard segment is expected to cause the segmented PU ionomer to possess some novel functions and improved physical properties, as reported on different molecular systems with primary focus being on antibacterium activity,[16] ionic conductivity,[17] high tensile modulus and tensile strength at room temperature,[15] and increased water vapor permeability.[14] To understand the role played by the total molecular weight and ionic groups within hard segment on the overall property of the copolymer, the first step is to elucidate the effect of ionic groups within hard segment on the crystallization of soft segment. To access the effectiveness of the shape memory effect, in practice, the copolymers are subjected to a testing routine, including the heating, deforming, and cooling of the sample. The testing cycle calls for a throughout understanding not only on the crystallinity and melting temperature of crystallization, but also on the crystallization rate and crystallizability. In this paper, a series of PCL-based segmented PU and the corresponding PU ionomers with different molecular weights were synthesized. The effect of molecular weight and ionic groups within hard segment on the crystallizability and melting behavior were studied with isothermal crystallization kinetics. The crystallization kinetics of PCL-based PU ionomers was investigated under isothermal conditions. Two parameters in the Avrami equation, n and K, depending on the nucleation details were determined for the PU nonionomers and ionomers. The activation energies for isothermal crystallization were then calculated accordingly.

EXPERIMENTAL

Sample preparation

PU nonionomers and ionomers were synthesized from polycaprolactone diols (PCL-4000), 4,4′-diphenylmethane diisocyanate (MDI), 1,4-butanediol (BD), and dimethylolpropionic acid (DMPA). The formulation of the PU samples is shown in Table I. PCL diols (Daicel Chemical Industries, Japan) with $M_w \sim$ 4000 were dried and degassed at 80°C under 1–2 mmHg for 24 h for PU synthesis. Extra pure grade of MDI (Kasei Kogyo, Tokyo, Japan), BD, and DMPA (Acros Organics, USA) were used to synthesize the PU samples. Triethylamine (TEA) (International Laboratory, USA) was used to neutralize the carboxy groups of DMPA. Dimethylformamide (DMF) is dehydrated with 4 Å molecular sieves for several days in advance, before using as solvent in PU synthesis. The PU samples

were then placed in a dry nitrogen atmosphere prior to use.

The reaction to prepare the prepolymer with PCL and MDI was carried out at 80°C for 2 h in a 500-mL round-bottomed, four-necked flask filled with nitrogen and equipped with a mechanical stirrer, a thermometer, and a condenser. Following the chain extension process with BD and/or DMPA for another 2 h, the neutralization reaction was carried out at 40°C for 1 h by adding stoichiometric amount of TEA agent. Segmented PU nonionomer and ionomer films were prepared by transferring some of the PU solution before or after neutralization to Teflon molds and allowed them to solidify at 60°C, in air for 24 h. To remove the residual DMF, the films were held at 75°C under vacuum of 1–2 mmHg for 24 h. The nominal thickness of the films was about 100 μm, measured by a Dektak profilometer.

In this study, the content of DMPA, soft segments, and the extent of neutralization in PU ionomer and nonionomer samples were adjusted to approximately the same values as shown in Table I to investigate the effect of ionic groups on the crystallization mechanism of PCL-4000-based PU with various M_w values. Molecular weight of the PU was determined by using gel permeation chromatography (GPC) (HEWLETT PACKARD 1050), with THF as the eluting solvent. The series of PU samples is designated as PU-XX, where XX denotes the number average molecular weight in kg/mol, a letter either representing nonionomers-"N" or ionomers-"I" is then followed. The soft segment content is calculated by assigning PCL-4000 units to the soft segment.

Differential scanning calorimetry measurement

The thermal properties of PU samples were investigated by DSC (PerkinElmer Diamond), purged with nitrogen gas, and cooled by liquid nitrogen. Indium and zinc standards were used for calibration. To ensure a consistent thermal history for the melting process, the samples were heated to 120°C and kept for 3 min. After that they were quenched to −100°C at a cooling rate of 200°C/min, then heated to 200°C at a rate of 20°C/min and the thermograms were recorded and compared.

Optical microscopy

A Leica polarizing optical microscope (POM) equipped with a Mettler FP 80 hot stage and a controller was used to observe the morphologies of PCL-4000, PU nonionomer and ionomer samples with the similar melting–crystallization cycles used in the isothermal crystallization process. The isothermal crystallization temperature in POM study is chosen to be at the room temperature (~20°C) which is approximately the T_c value (crystallization temperature) in the study of isothermal crystallization kinetics.

Isothermal crystallization

Isothermal crystallization experiments were performed using a PerkinElmer DSC-7. Pure water and Indium were used for the temperature calibration. The sample (~4–6 mg) was initially heated to 100°C at a rate of 10°C/min and held at 100°C for 5 min to remove the thermal history of the crystallizable phase, then it was rapidly cooled (60°C/min) to a designated crystallization temperature T_c, and it was held at this temperature to the end of the exothermic crystallization. The heat of fusion during the isothermal crystallization process was recorded as a function of time. The isothermal crystallization temperature and the cooling rate is chosen in accord with that of PCL-4000 and PU previously reported.[12,18] The crystallization of PCL-4000 is carried out in the temperature range from 25 to 42°C, while for PU ionomers and nonionomers with various M_w values, the temperature ranges from 15 to 25°C, in view of the large difference in crystallizability between PU and PCL-4000.

The amounts of heat generated during the development of crystal phase were recorded and analyzed, according to the usual equation of evaluating the relative degree of crystallinity X_t:

$$X_t = \frac{\int_{t_0}^{t} \left(\frac{dH}{dt}\right) dt}{\int_{t_0}^{t=\infty} \left(\frac{dH}{dt}\right) dt} \quad (1)$$

where t_0 and t_∞ are the time at which the sample reaches isothermal conditions (as indicated by a flat base line after an initial spike in the thermal curve) and the time at which the dominant sharp exothermic peak ends, respectively. H is the enthalpy of crystallization at time t. After isothermal crystallization, the sample was heated to 100°C and the melting temperature T_m indicated by the maximum of the endothermic peak was recorded.

RESULTS AND DISCUSSION

Differential scanning calorimetry measurement

As shown in Figure 1 and Table II, the glass transition temperature (T_g) of the soft segment increases with increase in the M_w value of the PU samples. It suggests that the more the hard segment dissolves in the soft domain the higher the restriction of soft segment mobility.[19–21] In view of the fact that the PU samples are of the same hard segment content, DMPA content, and molecular structure, the effect of the M_w value on the change of T_g is quite pronounced. It suggests that high molecular weight PU samples enhance the mixing process of soft and hard segments. It is observed that the change in the

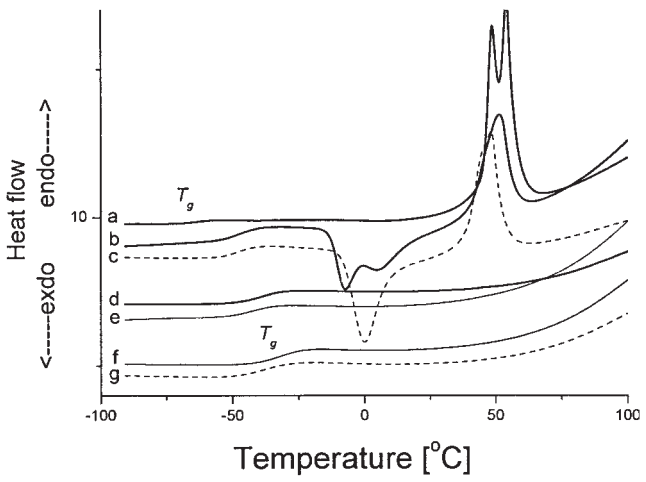

Figure 1 (a) DSC heating curves (20°C/min) of PCL-4000 after cooling at 200°C/min from 120°C, (b) PU-20N nonionomer, (c) PU-201 ionomer, (d) PU-58N nonionomer, (e) PU-58I ionomer, (f) PU-71N nonionomer, and (g) PU-71I ionomer.

heat capacity (ΔC_p) of PCL-4000 is smaller than that of the PU samples, which may be due to the existence of nonisothermal crystallization process participating in the cooling process of the PCL-4000. Therefore, the amount of amorphous phase having flexible molecular chain of PCL-4000 is decreased, resulting in smaller ΔC_p. The melting endothermal peak of the DSC curve of PCL-4000 is a signature of the crystallization process. In Table II, it is worth noting that both the T_g and ΔC_p values of the PU ionomers are smaller than that of the corresponding PU nonionomers. The drop of ΔC_p is direct evidence showing that the Coulombic forces between the ionic groups can restrict the soft segment mobility. On the other hand, from the decrease of T_g value after neutralizing the corresponding PU nonionomers, the improvement of the micro-phase separation especially in high molecular weight PU ionomers is observed. After neutralization of PU samples, for instance, PU-71N and PU-71I, the T_g of the soft segment is decreased substantially with the presence of ionic groups, suggesting that the Coulombic forces are responsible for the extension of microphase separation. These forces restrict largely the soft segments segregation for low molecular weight PU samples, resulting in lower T_g values. We conclude in this section that the effect of Coulombic forces is different on PU samples with different M_w values—they play different roles on the crystallization process in PU samples with different molecular weights. We shall show later that this unique effect manifests itself in the change in Avrami parameters, n and K, in isothermal crystallization.

From the DSC thermograms of PU-20N and PU-20I, there are two exdothermal recrystallization peaks at about −10 and 0°C, respectively. However, for the thermograms of PU-20N and PU-20I as shown in Figure 1(b, c), not only the peak position but also the peak shape is totally different, suggesting that the crystallization rate and crystallization mechanism have been altered by neutralization. As the molecular weight increases, the DSC thermograms in Figure 1(d–g) for samples PU-58N, PU-58I, PU-71N, and PU-71I shows decreased PU crystallizability, resulting in no significant exdothermal recrystallization and melting features.

Morphology of the soft segment crystal in polyurethane

Figure 2 shows the crystal morphologies of PCL-4000. The nominal crystal size shown in the figure is about 30–50 μm, which is consistent with the literature reported.[9] In general, both the average crystal sizes of PU nonionomers and ionomers decrease with increasing M_w compared with that of PCL-4000. However, the evolution of crystal morphology for each pair of PU nonionomer and ionomer samples with the same M_w value is different. For instance, in the case of PU-20N/PU-20I, which falls into the low M_w regime, the crystal size in PU-20N is smaller while the crystal outlook still resembles roughly the morphological details as in PCL-4000. This is an illustration of the effect of ionic groups in hard segments on the crystal size and in turn the crystal morphology in PU. The pair of PU samples denoted by PU-58N/PU-58I shares a similar surface morphology. Their crystal sizes in PU are nearly the same but originated from a different morphological transformation. The last pair of samples (PU-71N/PU-71I) has the highest M_w value, but their crystal sizes are the smallest among all the other PU films. The difference in morphological transformation suggests the different effects played by the Coulombic forces on the crystallization

TABLE II
Thermal Properties of PCL and PU Samples

	T_g (°C)	ΔC_p (J/g °C)	$T_{(end)}$ (°C)	$T_{(onset)}$ (°C)	$T_{(end)} - T_{(onset)}$
PCL-4000	−65.81	0.056	−61.18	−70.12	8.94
PU-20N	−46.40	0.303	−39.35	−55.21	15.86
PU-20I	−46.71	0.285	−39.92	−54.87	14.95
PU-58N	−41.29	0.208	−34.95	−47.27	12.32
PU-58I	−43.86	0.176	−37.18	−50.97	13.79
PU-71N	−32.00	0.205	−24.3	−40.01	15.71
PU-71I	−39.46	0.203	−30.64	−47.96	17.32

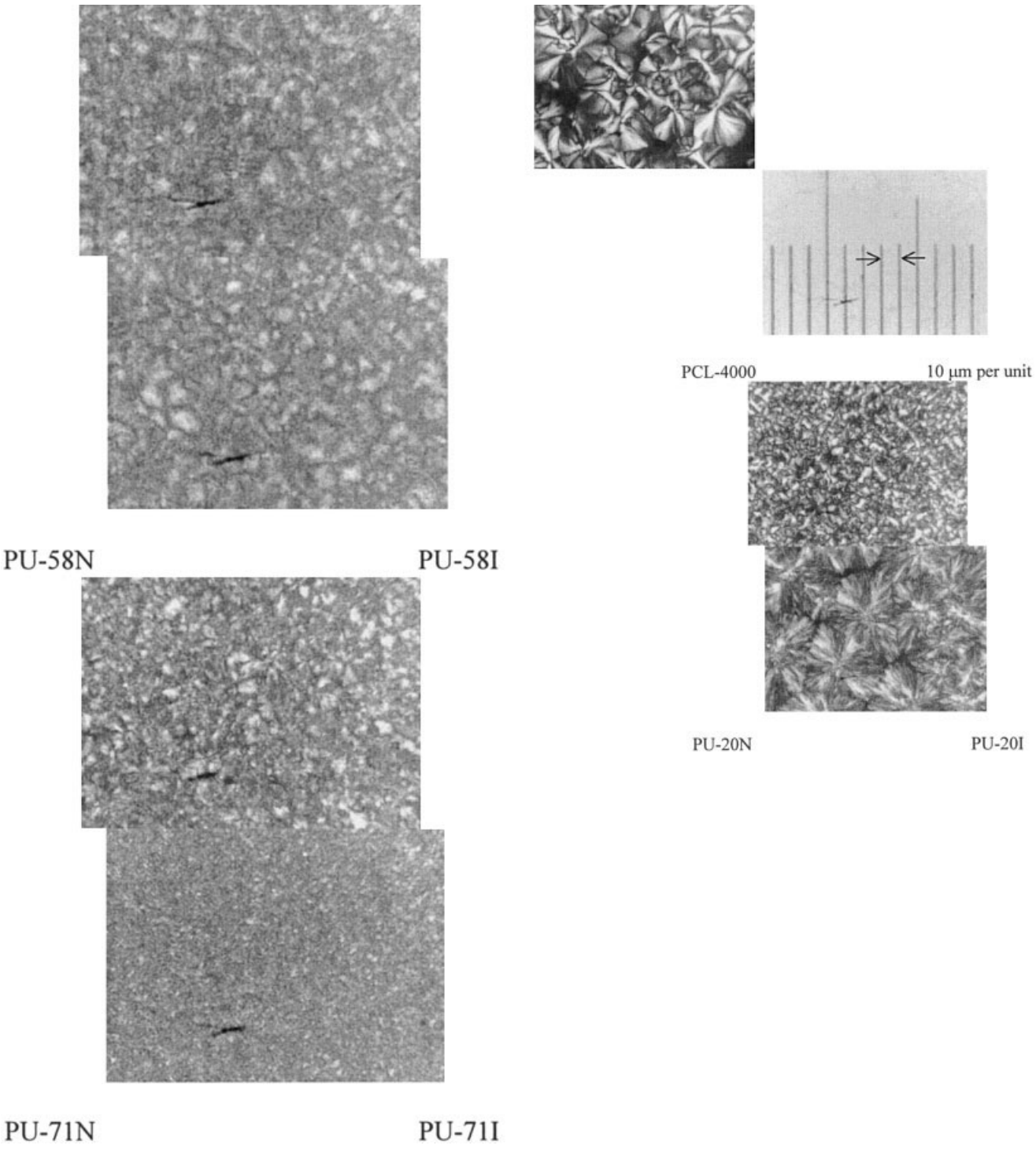

Figure 2 POM images of the crystals for PCL-4000 and PU nonionomers and ionomers with different molecular weights.

process. This opens up a new line of research on the perturbation of crystallization kinetics analysis of such copolymer.

Analysis of isothermal crystallization kinetics

The overall kinetics of the isothermal crystallization from the melt can be analyzed on the basis of the Avrami equation.[22] This crystallization theory is widely accepted to describe the physical behavior of a variety of crystallization process, for instance, semicrystallization in polymer, polymer blends, and copolymers.[23–28] We use the modified Avrami equation called the Ozawa equation to describe the crystallization kinetics:

$$X(t) = 1 - \exp(-Kt^n) \quad (2)$$

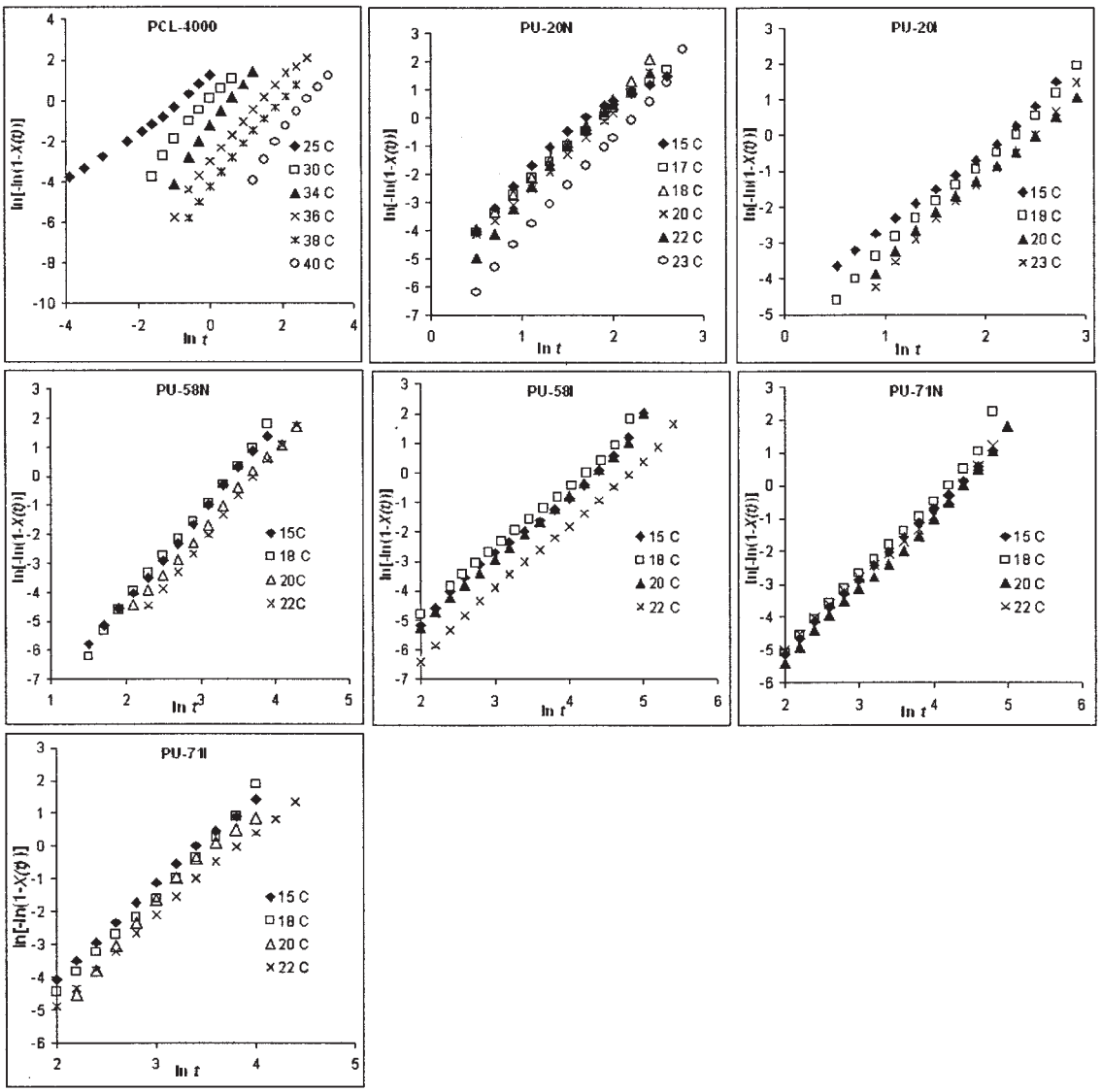

Figure 3 Plots of $\ln[-(\ln(1 - X(t))]$ against $\ln t$ for isothermal crystallization with various temperatures.

which can be linearized in the form:

$$\ln[- \ln(1 - X(t))] = n\ln t + \ln K \quad (3)$$

where n is the Avrami (Ozawa) exponent whose value depends upon the mechanism of nucleation and on the crystal-growth geometry, K is a rate constant containing the nucleation and the growth parameters. Theoretically, if eq. (3) can adequately follow the crystallization process, a plot of $\ln[-\ln(1 - X(t))]$ against $\ln t$ should yield a straight line with slope n and intercept $\ln K$.

The double logarithmic plots of $\ln[-\ln(1 - X(t))]$ against $\ln t$ for PCL-4000, nonionomers, and ionomers with various temperatures are shown in Figure 3. Each plot represents a linear dependence of $\ln[-\ln(1 - X(t))]$ on $\ln t$, but with slight deviation from the predicted, when both parameters are large, indicating the existence of a secondary crystallization of PCL that occurs consecutively with primary. The study of PCL (M_w = 80,000) by Kuo et al.[29] suggests that the PCL with a higher M_w value has the same tendency at a later stage in the crystallization process. The deviation is attributed to the secondary crystallization involving fibrillar growth between the primary lamellae of the spherulite, and leading to the occurrence of spherulite impingement.

The values of n and K for a particular sample can be determined from the initial linear portions of the double logarithmic plots shown in Figure 3. The results for different samples are summarized in Table III. The Avrami parameter n of PCL-4000 at 40°C in our experiment is consistent to that reported by Bogdanow et al.[12] For PCL-4000, the Avrami parameter n is ~1–2 and 3–4 at low and high crystallization temperatures,

TABLE III
The Avrami Parameters *n*, *K*, *t*(0.5) (Crystallization Half Time), and *E* (Activation Energy) of the Soft Segment of PU Nonionomers and Ionomers Based on PCL-4000

	M_w	T_c (°C)	T_c (K)	N	ln K	K	$1/T_c$	$(1/n)$ ln K	ΔE (kJ/mol)	t(0.5) (min)	[a]$K=\ln 2/[t(0.5)]^n$	ln K
PCL-4000	4000	25	298.15	1.28	1.060	2.89 E +00	3.35 E −03	0.83	184.09	0.355	2.61 E +00	0.959
		30	303.15	2.12	0.037	1.04 E +00	3.30 E −03	0.02		0.760	1.24 E +00	0.215
		34	307.15	2.46	−1.360	2.57 E −01	3.26 E −03	−0.55		1.440	2.83 E −01	−1.264
		36	309.15	2.09	−3.120	4.42 E −02	3.23 E −03	−1.49		3.470	5.17 E −02	−2.963
		38	311.15	2.17	−4.240	1.44 E −02	3.21 E −03	−1.95		5.960	1.44 E −02	−4.240
		40	313.15	2.42	−6.520	1.47 E −03	3.19 E −03	−2.69		11.950	1.71 E −03	−6.370
		42	315.15	4.26	−12.750	2.90 E −06	3.17 E −03	−2.99		19.400	2.27 E −06	−12.994
PU-20N	20200	15	288.15	3.29	−5.432	4.37 E −03	3.47 E −03	−1.65	36.80	4.650	4.40 E −03	−5.427
		17	290.15	3.01	−5.535	3.95 E −03	3.45 E −03	−1.84		5.670	3.74 E −03	−5.589
		18	291.15	3.08	−5.504	4.07 E −03	3.43 E −03	−1.79		5.320	4.06 E −03	−5.506
		20	293.15	2.87	−5.613	3.65 E −03	3.41 E −03	−1.96		6.120	3.83 E −03	−5.566
		22	295.15	3.75	−6.766	1.15 E −03	3.39 E −03	−1.80		5.500	1.15 E −03	−6.766
		23	296.15	3.35	−7.436	5.90 E −04	3.38 E −03	−2.22		8.230	5.90 E −04	−7.436
		25	298.15	2.91	−6.413	1.64 E −03	3.35 E −03	−2.20		7.900	1.68 E −03	−6.387
PU-20I	20200	15	288.15	2.18	−4.778	8.41 E −03	3.47 E −03	−2.20	28.53	7.830	7.87 E −03	−4.844
		18	291.15	2.32	−5.345	4.77 E −03	3.43 E −03	−2.30		8.630	4.63 E −03	−5.376
		20	293.15	2.23	−5.563	3.84 E −03	3.41 E −03	−2.49		10.500	3.62 E −03	−5.622
		23	296.15	2.42	−6.023	2.42 E −03	3.38 E −03	−2.49		10.530	2.33 E −03	−6.061
PU-58N	58500	15	288.15	3.12	−10.637	2.40 E −05	3.47 E −03	−3.41	34.02	26.683	2.48 E −05	−10.603
		18	291.15	3.09	−10.480	2.80 E −05	3.43 E −03	−3.40		26.490	2.79 E −05	−10.485
		20	293.15	2.92	−10.670	2.33 E −05	3.41 E −03	−3.65		33.340	2.48 E −05	−10.603
		22	295.15	3.21	−11.930	6.62 E −06	3.39 E −03	−3.71		36.110	6.88 E −06	−11.887
PU-58I	58500	15	288.15	2.00	−8.783	1.53 E −04	3.47 E −03	−4.39	39.70	67.890	1.51 E −04	−8.801
		18	291.15	2.07	−8.760	1.56 E −04	3.43 E −03	−4.23		58.420	1.52 E −04	−8.795
		20	293.15	2.18	−9.510	7.43 E −05	3.41 E −03	−4.36		66.100	7.40 E −05	−9.512
		22	295.15	2.13	−10.300	3.36 E −05	3.39 E −03	−4.83		104.970	3.42 E −05	−10.282
PU-71N	71600	15	288.15	2.16	−9.358	8.62 E −05	3.47 E −03	−4.33	12.90	63.975	8.63 E −05	−9.358
		18	291.15	2.27	−9.516	7.36 E −05	3.43 E −03	−4.19		57.290	7.12 E −05	−9.550
		20	293.15	2.23	−9.880	5.14 E −05	3.41 E −03	−4.43		69.900	5.39 E −05	−9.830
		22	295.15	2.03	−8.955	1.29 E −04	3.39 E −03	−4.41		68.940	1.28 E −04	−8.965
PU-71I	71600	15	288.15	2.71	−9.334	8.84 E −05	3.47 E −03	−3.44	31.13	26.020	1.01 E −04	−9.197
		18	291.15	2.96	−10.390	3.07 E −05	3.43 E −03	−3.52		29.790	3.05 E −05	−10.396
		20	293.15	3.48	−12.150	5.29 E −06	3.41 E −03	−3.49		30.180	4.91 E −06	−12.220
		22	295.15	2.63	−10.028	4.41 E −05	3.39 E −03	−3.81		38.270	4.70 E −05	−9.966

[a] The crystallization rate parameter K is derived from eq. (4).

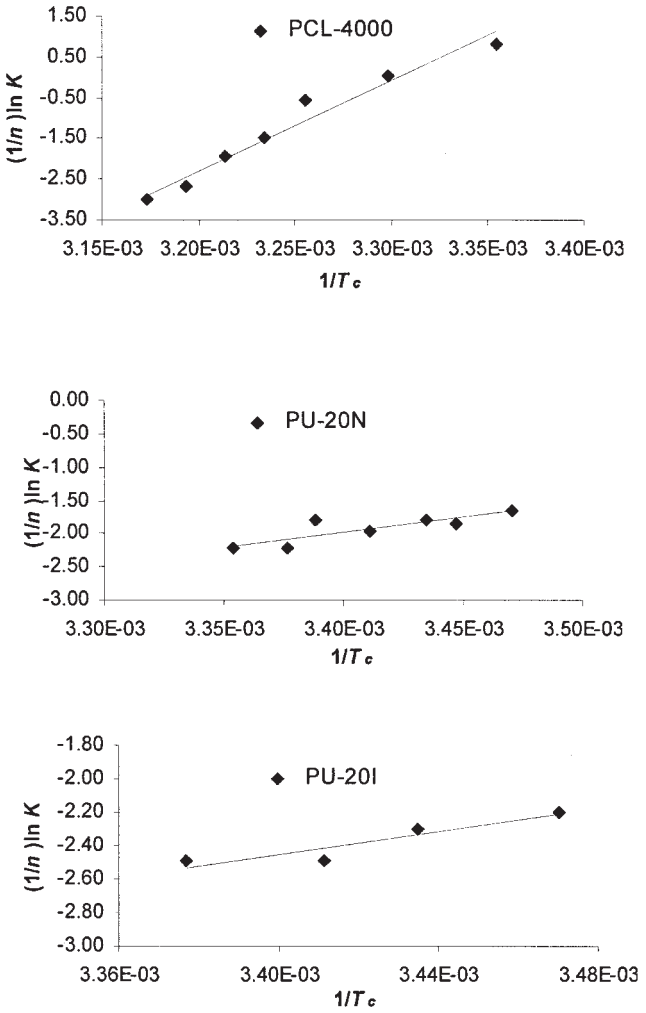

Figure 4 Plots of (l/n) ln K against l/T_c from isothermal crystallization.

respectively. The isothermal crystallization of PU can be described by the Avrami equation with the exponent n ranging from 2 to 3 at the crystallization temperature chosen in this study. However, it has been observed that ionic group in hard segments plays a significant role in altering the crystallization mechanism in PU films. The Avrami parameter n is decreased from 3 to 2 after neutralization process in PU samples with lower M_w values, such as PU-20I and PU-58I, but increased from 2 to 3 in samples with higher M_w values, such as PU-71I. This is a manifestation of a different crystallization mechanism induced by the ionic groups in PCL-4000-based PU with different M_w values. An understanding of the M_w dependence of the Avrami parameters is slightly more involved. In PU samples with lower M_w, the extent of the soft and hard segment phase mixing is relatively not very high compared with that in high M_w samples. Under this circumstance, the effect of ionic groups in the hard segments on the microphase separation is not effective. However, the increased hard segment cohesive force induced by the ionic groups after neutralization may bring about restriction on the physical mobility of soft segment, resulting in the decrease and increase of the Avrami parameters n and K, respectively. In PU samples with higher M_w values, the extent of phase mixing is expected to be higher. The Coulombic forces between ionic groups improve the microphase separation significantly. The crystallization mechanism is then altered and can be observed by the reversed change in the Avrami parameters n and K.

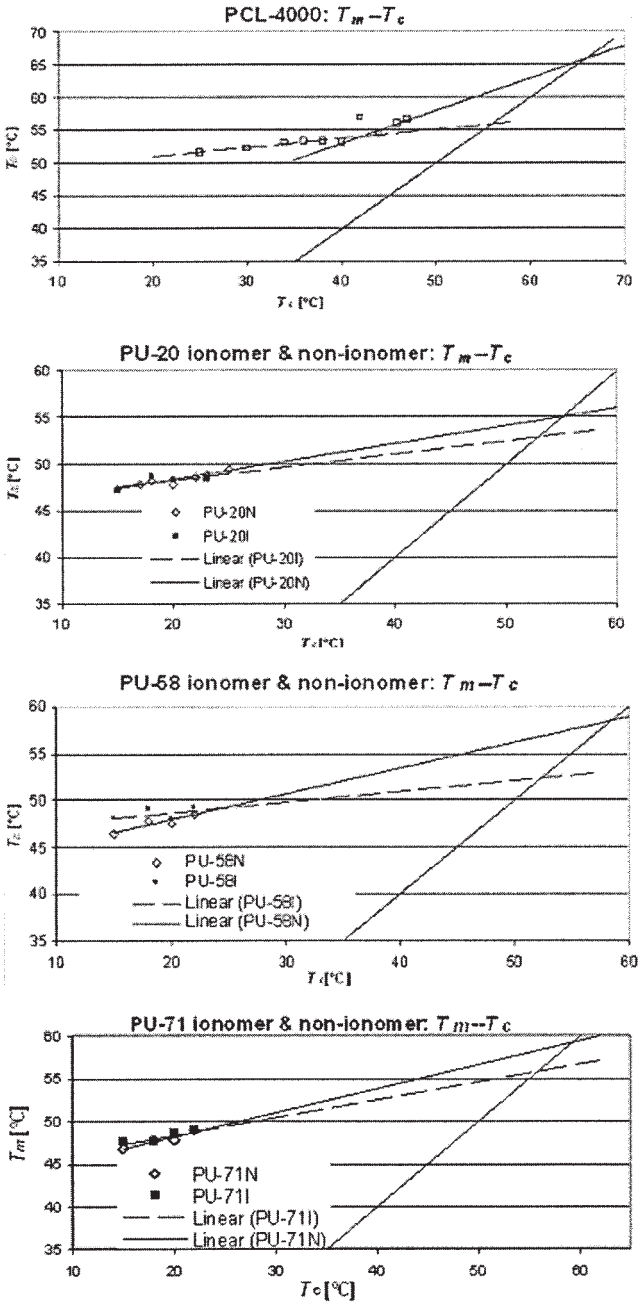

Figure 5 Plots of the observed melting temperature T_m against T_c for PU ionomer and nonionomers with different molecular weights.

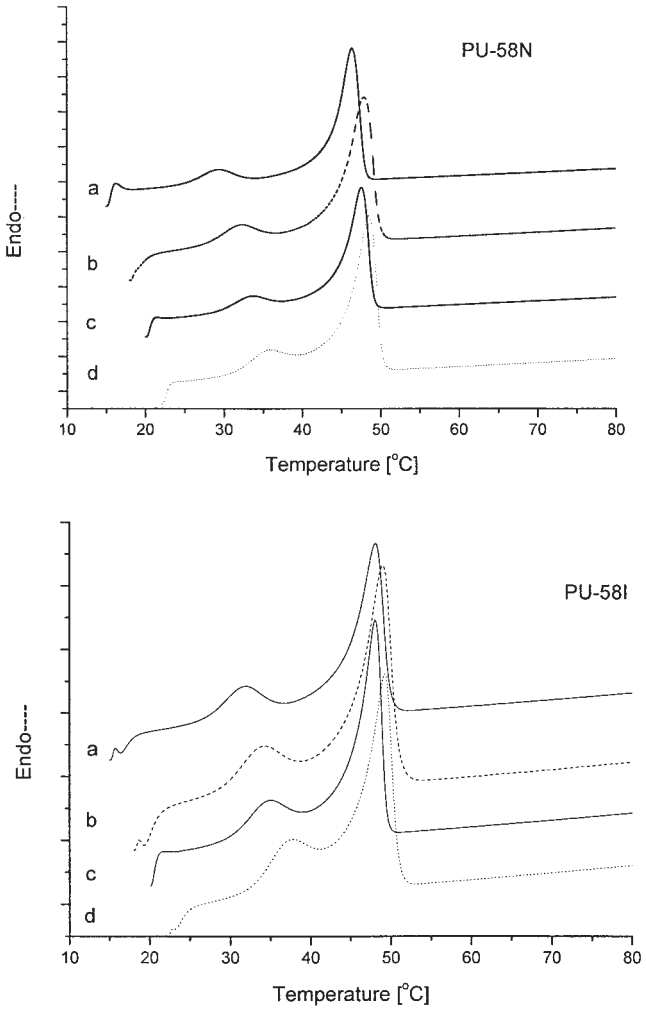

Figure 6 DSC thermograms of sample PU-58N (upper) and PU-58I (lower) after isothermal crystallization at (a) T_c = 15°C, (b) T_c = 18°C, (c) T_c = 20°C, and (d) T_c = 22°C.

The half crystallization time $t(0.5)$ is defined as the time at which the crystallinity is equal to 50%. It is related to the Avrami parameter K and can be determined from the following expression:

$$K = \ln 2/[t(0.5)]^n \tag{4}$$

Table III summarizes the Avrami parameters for the soft segments of PU nonionomers and ionomers. The parameter K calculated from eq. (4) agrees well with that obtained experimentally and is summarized in Figure 3. It suggests that the Avrami equation analysis is adequate to describe the crystallization mechanism of PCL-4000-based PU ionomers and nonionomers.[30] Usually, the rate of crystallization is mathematically defined as the inverse of $t(0.5)$. The values of $t(0.5)$ for different samples are summarized in Table III. It illustrates the fact that in PU samples having low M_w values, such as PU-20 and PU-58, the crystallization rate ($1/t(0.5)$) is decreased by the presence of ionic groups. On the contrary, in PU samples having high M_w values, such as PU-71, the presence of ionic groups promotes the crystallization process. This shows that the role of ionic groups in samples with different M_w values is different.

Analysis of crystallization activation energy

The crystallization process in PCL-4000 or soft segments of PU is assumed to be thermally activated. The Avrami paprmeter K can then be described by the Arrhenius equation[23–28]:

$$K^{1/n} = k_0 \exp\left(-\frac{\Delta E}{RT_c}\right) \tag{5}$$

or

$$(1/n)\ln K = \ln k_0 - \frac{\Delta E}{RT_c} \tag{6}$$

where k_0 is a temperature-independent preexponential factor, R is the gas constant, and ΔE is the crystallization activation energy (in kJ/mol). The plots of the parameter $(1/n)$ ln K against the inverse of the corresponding T_c for the PCL-4000, PU nonionomer and ionomer samples are shown in Figure 4. The activation energy is calculated and summarized in Table III. For PCL-4000, the ΔE for the primary crystallization process is calculated to be −183.09 kJ/mol, while for PU nonionomer (PU-20N) and ionomer (PU-20I) samples, the ΔE increases significantly to −36.80 and −28.53 kJ/mol, respectively. Comparison of the activation energy for different samples indicates that the ionic groups have less influence on the ΔE in PU samples with low M_w values. On the contrary, for PU samples having high M_w values, such as PU-71I, the ΔE is decreased from −12.9 to −31.13 kJ/mol after neutralization by TEA.

Equilibrium melting temperature

A dominant sharp exothermic peak in the reheating DSC thermogram of our samples is considered to be the primary melting temperature (T_m). Figure 5 clearly reveals that T_m increases linearly with T_c. The experimental data can be fitted well by the Hoffman–Weeks equation[31]:

$$T_m = \phi T_c + (1 - \phi)T_e \tag{7}$$

where T_e is the equilibrium melting point, and $\Phi = 1/\gamma$ is the stability parameter depending on the crystal thickness (γ is the ratio of the lamellar thickness L to the lamellar thickness of the critical nucleus L^* at T_c). The Φ in eq. (7) can have values between 0

TABLE IV
Values of the Equilibrium Melting Temperature T_e, the Stability Parameter Φ, and the Lower and Higher Apparent Melting Temperature of PU Sample

	T_c (°C)	$T_{m\text{-}1}$ (°C)[a]	$T_{m\text{-}2}$ (°C)[a]	T_e (°C)	Φ
PCL-4000	25.00		51.62	65.89	0.50
	30.00		52.21		
	34.00		53.00		
	36.00		53.31		
	38.00		53.25		
	40.00		53.05		
	42.00		56.87		
	44.00		54.50		
	46.00		56.03		
	47.00		56.53		
PU-20N	15.00	25.49	47.34	55.07	0.19
	17.00	28.01	47.83		
	18.00	29.19	48.17		
	20.00	30.86	47.81		
	22.00	32.52	48.63		
	23.00	33.68	48.94		
	25.00	35.35	49.42		
PU-20I	15.00	26.15	47.16	52.83	0.14
	18.00	29.17	48.67		
	20.00	30.34	48.31		
	23.00	33.00	48.43		
PU-58N	15.00	29.34	46.34	58.51	0.28
	18.00	32.34	47.84		
	20.00	33.67	47.50		
	22.00	36.00	48.50		
PU-58I	15.00	31.84	48.00	52.36	0.11
	18.00	34.17	49.00		
	20.00	35.00	48.00		
	22.00	37.84	49.17		
PU-71N	15.00	32.00	46.84	59.32	0.28
	18.00	34.67	47.84		
	20.00	36.67	47.84		
	22.00	38.84	49.00		
PU-71I	15.00	31.00	47.50	55.89	0.21
	18.00	33.17	47.50		
	20.00	36.10	48.53		
	22.00	38.00	48.84		

and 1 ($\Phi = 0$ and $T_m = T_e$, whereas $\Phi = 1$ and $T_m = T_c$). The crystal are most stable for $\Phi = 0$ and unstable for $\Phi = 1$. T_e can be calculated from the intersection point between plots of T_m against T_c and lines of $T_m = T_c$.

As shown in Figure 5, the melting temperature T_m for PCL-4000- and PCL-4000-based PU samples increases with the crystallization temperature T_c as expected. The extrapolation of the observed melting temperatures to the line $T_m = T_c$ has been widely employed to calculate the T_e of different copolymers and homopolymers.[19] However, in the case of the study on segmented poly(ester-urethanes) based on poly(ε-caprolactone) by Bogdanow et al.,[12] linear polyethylene and random copolymers at low level of crystallinity by Alamo et al.,[32,33] this extrapolation method fails to describe the relations between the T_m and T_c. Bogdanow et al. have used different approaches to understand this scenario.[12] First, the nonisothermal crystallization during cooling to certain T_c causes the corresponding T_m to increase. Second, the observed dependence also arises from annealing during the heating scan which causes the improvement in crystal quality and hence the T_m increases, and the effect is particularly pronounced when T_c is lower. Therefore, in our investigation of T_e of PCL-4000, the equilibrium melting temperature is calculated from the crystallization temperatures range above 38°C. As a result, T_e for PCL-4000 is 65.89°C, which is in agreement with the literature reported.[12,18]

It is worth noting that there are double-melting features in all the DSC thermograms shown in Figure 6. Similar signature was also observed on the 30/70 DGEBA/PCL blend, binary blends of solution-chlori-

nated polyethylenes (CPE) with polycaprolactone (PCL), and blends of poly(hydroxyl ether of bisphenol A) (Phenoxy) with polycaprolactone (PCL).[34–36] In the investigation on Phenoxy/PCL by Defieuw,[36] the isothermal crystallization process was interrupted after different time intervals and DSC melting trace was immediately recorded. The highest melting endotherm reaches a constant area and position on the temperature scale after short isothermal crystallization times (primary crystallization), while the lower melting peak only appears after much longer crystallization times (secondary crystallization). The secondary crystallization is supposed to occur in the amorphous phase segregated during the primary crystallization of PCL, resulting in a slower crystallization process as this happens in the presence of a higher Phenoxy concentration. Therefore, in calculation of the equilibrium melting temperature of PCL-4000-based PU ionomers and nonionomers, the higher melting temperature corresponding to the primary crystallization was used.

Table IV summarizes the values of equilibrium melting temperature (T_e) of all the PU samples. It is interesting to note that the T_e values of PU samples are lower than that of PCL-4000 and increase with increasing the molecular weight of the PU samples. After neutralization, it is observed that the T_e values of the PU ionomers are decreased. The stability parameter Φ varies within 0.28 to 0.11 in PU samples, suggesting that the formation of crystals in PU samples is rather stable. The Φ values of PU ionomers samples are significantly smaller than the corresponding PU nonionomers, providing clear evidence that the ionic groups in hard segments improve the stability of the crystallization in soft segment. Finally, the Φ value of PCL-4000 is larger than that in all the PU ionomers and nonionomers, which can be attributed to the relative larger critical lamellar thickness L^* value of PCL-4000.

CONCLUSIONS

We have synthesized the PCL-4000-based PU nonionomers and their corresponding ionomers having different M_w values. The crystallization kinetics of the above samples were examined and compared with that of PCL-4000, suggesting that ionic groups in hard segments play different roles on the crystallization of soft segments in PU samples with different M_w values. In PU samples having low M_w values, the Coulombic forces restrict the physical mobility of the molecular chains and bring about the decrease and increase in the Avrami parameter n and K, respectively. On the contrary, the Coulombic forces can promote the microphase separation in PU samples with high M_w values, resulting in the increase in n but decrease in K. Accordingly, the crystallization rate is lowered in PU having low M_w values but is higher in samples with high M_w values. Our results suggest that the crystallization process compared with the corresponding PU nonionomer is affected significantly by the Coulombic forces in the hard segments portion of the PU ionomer, which in turn is believed to have direct impact on the shape memory effect on this special class of polyurethane. The research in this aspect is underway and will be reported elsewhere.

References

1. Hu, J. L.; Yang, Z.; Yeung, L.; Ji, F. L.; Liu, Y. Polym Int, 2005, 54, 854.
2. Hu, J. L.; Ji, F. L.; Wong, Y. W. Polym Int, 2005, 54, 600.
3. Hu, J. L.; Mondal, S. Polym Int, 2005, 54, 764.
4. Ota, S. Radiat Phys Chem 1981, 18, 81
5. Hayashi, S. Plast Sci 1989, 173 (in Japanese).
6. Lendlien, A.; Kelch, S. Angew Chem Int Ed 2002, 41, 2034.
7. Tobushi, H.; Hashimoto, T.; Ito, N. J Intell Mater Syst Struct 1998, 9, 127.
8. Wei, Z. G.; Sandström, R.; Miyazaki, S. J Mater Sci 1998, 33, 3743.
9. Lee, H. Y.; Jeong, H. M.; Lee, J. S.; Kim, B. K. Polymer J 2000, 32, 23.
10. Li, F. K.; Zhang, X.; Hou, J. A.; Zhu, W.; Xu, M. Acta Polym Sin 1996, 4, 462.
11. Li, F. K.; Chen, Y.; Zhu, W.; Zhang, X.; Xu, M. Polymer 1998, 39, 6929.
12. Bogdanow, B.; Toncheva, V.; Schacht, E.; Finelli, L.; Sarti, B.; Scandola, M.; Polymer 1999, 40, 3171
13. Jeong, H. M.; Ahn, B. K.; Cho, S. M.; Kim, B. K. J Polym Sci Part B: Polym Phys 2000, 38, 3009.
14. Jeong, H. M.; Ahn, B. K.; Kim, B. K. Polym Int 2000, 49, 1714.
15. Kim, B. K.; Lee, S. Y.; Lee, J. S.; Baek, S. H.; Choi, Y. J.; Lee, J. O.; Xu, M. Polymer 39 1998, 13, 2803.
16. Yang, J. E.; Kong, J. S.; Park, S. W.; Lee, D. J.; Kim, H. D. J Appl Polym Sci 2002, 86, 2375.
17. Wei, X.; Yu, X. H. J Polym Sci Part B: Polym Phys 1997, 35, 225.
18. Cheng, H. L.; Li, L. J.; Ou-Yang, W. C.; Hwang, J. C.; Wong, W. Y. Macromolecules 1997, 30, 1718.
19. Liu, Y.; Pan, C. Y. Eur Polym J 1998, 34, 621.
20. Sanchez-Adsuar, M. S. Int J Adhes Adhes 2000, 20, 291.
21. Garrett, J. T.; Xu, R.; Cho, J.; Runt, J. Polymer 2003, 44, 2711.
22. Avrami, M. J Chem Phys 1939, 7, 1103.
23. Liu, S. Y.; Ning, Y.; Cui, Y.; Zhang, H. F.; Mo, Z. S. J Appl Polym Sci 1998, 70, 2371.
24. Li, C.; Jian, G. H.; Zhang, Y.; Zhang, Y. X. Polym Test 2002, 21, 919.
25. Kim, S. H.; Ahn, S. H.; Hirai, T. Polymer 2003, 44, 5625.
26. Alwattari, A. A.; Lloyd, D. R. Polymer 1998, 39, 1129.
27. Lin, C. C. Polym Eng Sci 1983, 23, 113.
28. Cebe, P. Hong, S. D.; Polymer 1986, 27, 1183.
29. Kuo, S. W.; Chan, S. C.; Chang, F. C. J Polym Sci Part B: Polym Phys 2004, 42, 17.
30. Li, J.; Zhou, C. X.; Wang, G.; Tao, Y.; Liu, Q.; Li, Y.; Polym Test 2002, 21, 583.
31. Hoffman, J. D.; Weeks, J. J. J Chem Phys 1962, 37, 1723.
32. Alamo, R. G.; Viers, B. D.; Mandelkern, L. Macromolecules 1995, 28, 3205.
33. Alamo, R. G.; Chan, F. K. M.; Mandelkern, L.; Macromolecules 1992, 25, 6381.
34. Guo, Q. P.; Groeninckx, G. Polymer 2001, 42, 8647.
35. Defieuw, G.; Groeninckx, G.; Reynaers, H. Polymer 1989, 30, 2164.
36. Rim, P. B.; Runt, J. P. Macromolecules 1983, 16, 762.